Journal of Power Sources 219 (2012) 292–304

Contents lists available at SciVerse ScienceDirect

Journal of Power Sources

journal homepage: www.elsevier.com/locate/jpowsour

# Control performance standards based load-frequency controller considering redox flow batteries coordinate with interline power flow controller

I.A. Chidambaram*, B. Paramasivam

*Department of Electrical Engineering, Annamalai University, Annamalainagar 608002, Tamilnadu, India*

## HIGHLIGHTS

- Redox flow batteries coordinate with IPFC on Load Frequency Control investigated.
- BFO algorithm is used to optimizing the controller design parameters.
- Control Performance Standard based controller reduction wear and tear of equipment.
- Simulation result gives coordinate control improves dynamic quality of Power system.

## ARTICLE INFO

*Article history:*
Received 12 April 2012
Received in revised form
6 June 2012
Accepted 6 June 2012
Available online 24 July 2012

*Keywords:*
Bacterial foraging optimization
Redox flow batteries
Interline power flow controller
Load-frequency control
Control performance standards

## ABSTRACT

This paper proposes a sophisticate application of redox flow batteries (RFB) coordinate with Interline Power Flow Controller (IPFC) for the improvement of Load Frequency Control (LFC) of a multiple units two- area power system. The Interline Power Flow Controller is to stabilize the frequency oscillations of the inter-area mode in the interconnected power system by the dynamic control of tie-line power flow. The redox flow batteries, which are not aged to the frequent charging and discharging, have a quick response and outstanding function during overload conditions. In addition to leveling load, the battery is advantageous for secondary control in the power system and maintenance of power quality of distributes power resources. The Bacterial Foraging Optimization (BFO) algorithm is use to optimize the parameters of the cost functions for designing the integral controller. Compliance with North American Electric Reliability Council (NERC) standards for Load Frequency Control has also been establishes in this work. Simulation studies reveal that the RFB coordinate with IPFC units has greater potential for improving the system dynamic performance.



## 1. Introduction

In an interconnected power system, a sudden load perturbation in any area causes the deviation of frequencies of all the areas and also of the tie-line powers. This has to be corrected to ensure generation and distribution of electric power with good quality. This is achieved by Load Frequency Control, also known as Automatic Generation Control (AGC). The main objectives of AGC [1,2] are to be maintain the desired megawatt output and the nominal frequency in an interconnected power system besides maintaining the net interchange of power between control areas at predetermined values. The paper proposes a control scheme that ensures reliability and quality of power supply, with minimum transient deviations and ensures zero steady state error. The importance of decentralize controllers for multi area load-frequency control system, where in, each area controller uses only the local states for feedback, is well known. The stabilization of frequency oscillations in an interconnected power system becomes challenging when implements in the future competitive environment. So advanced economic, high efficiency and improved control schemes [3,4] are required to ensure the power system reliability. The conventional load-frequency controller may no longer be able to attenuate the large frequency oscillation due to the slow response of the governor [5]. The recent advances in power electronics have led to the development of the Flexible Alternating Current Transmission Systems (FACTS). These FACTS devices are capable of controlling the network condition in a very fast manner [6] and because of this reason the usage of FACTS devices are more apt to improve the stability of power system. Several FACTS devices, such as Thyristor Controlled Series Capacitor (TCSC), STATic synchronous COMpensator (STATCOM), Thyristor Controlled Phase Shifter (TCPS), Static Synchronous

* Corresponding author. Tel.: +91 9842338501; fax: +91 4144238080.
*E-mail addresses:* driacdm@yahoo.com (I.A. Chidambaram), bpssivam@gmail.com (B. Paramasivam).

0378-7753/$ – see front matter © 2012 Elsevier B.V. All rights reserved.
http://dx.doi.org/10.1016/j.jpowsour.2012.06.048

Series Compensator (SSSC), Unified Power Flow Controller (UPFC), Interline Power Flow Controller (IPFC), have been developed in recent decades [7]. An Interline Power Flow Controller consists of a set of converters that are connected in series with different transmissions lines which can effectively manage the power flow control in multi line systems. The schematic diagram of IPFC is illustrated in Fig. 1. The Unified Power Flow Controller and Interline Power Flow Controller consists at least two converters. It is found that, in the past, much effort has been made in the modeling of the UPFC to compensate a single transmission line for power flow analysis [8–10], whereas the IPFC is conceived for the compensation and power flow management of multi-line transmission system. Therefore, UPFC is not attractive for compensating multi-line systems from economical point of view [11]. Interline Power Flow Controller not only can compensate each transmission line separately but also can compensate all of them at the same time. It employs a number of Voltage Source Converters (VSC) linked at the same DC terminal; each of them can provide series compensation for its own line [12]. In this way, the power optimization of the overall system can be obtain in the form of appropriate power transfer through the common DC link from over-loaded lines to under-loaded lines [13]. A simple model of IPFC with optimal power flow control method to solve overload problem and the power flow balance for the minimum cost [14] has been proposed.

In this paper Interline Power Flow Controller is being install in the tie-line between any interconnected areas, which is use to stabilize the area frequency oscillations by high speed control of tie-line power through the interconnections. In addition it can also be expect that the high speed control of IPFC can be coordinate with slow speed control of governor system for enhancing stabilization of area frequency oscillations effectively. Under these situations, the governor system may no longer be able to absorb the frequency fluctuations. In order to compensate for sudden load changes, an active power source with fast response such as redox flow batteries is expect as the most effective counter measure. The redox flow batteries will, in addition to load leveling, a function conventionally assigned to them, have a wide range of applications such as power quality maintenance for decentralized power supplies. The redox flow batteries are the excellent short-time overload output and the response characteristics possessed in the particular [15,16]. The effect of generation control and the absorption of power fluctuation required for power quality maintenance are expected, however it will be difficult to locate the placement of RFB alone in every possible area in the interconnected system due to the economical reasons. Therefore RFB coordinate with IPFC are capable of controlling the network conditions in a very fast and economical manner.

Nowadays power system complex are being solved with the use of Evolutionary Computation (EC) such as Differential Evolution (DE) [17], Genetic Algorithms [GA], Practical Swarm Optimizations [PSO] [18], Ant Colony Optimization [ACO] [19], which are some of the heuristic techniques having immense capability of determining

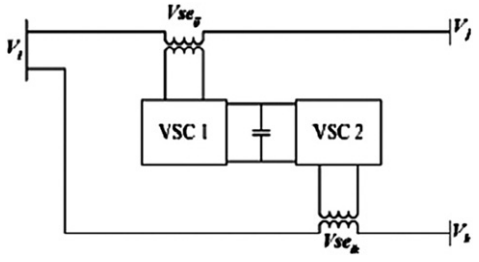


**Fig. 1.** Schematic diagram IPFC.

global optimum. Classical approach based optimization for controller gains is a trial and error method and extremely time consuming when several parameters have to be optimized simultaneously and provides suboptimal result [18,19]. Some authors have applied GA to optimize controller gains more effectively and efficiently than the classical approach. But the premature convergence of GA degrades its search capability. Recent research has brought out some deficiencies in using GA, PSO based techniques [20,21]. The Bacterial Foraging Optimization [BFO] mimics how bacteria forage over a landscape of nutrients to perform parallel non gradient optimization [22]. The BFO algorithm is a computational intelligence based technique that is not large affected by the size and non-linearity of the problem and can be convergence to the optimal solution in many problems where most analytical methods faith convergence. A more recent and powerful evolutionary computational technique BFO [23] is found to be user friendly and is adopted for simultaneous optimization of several parameters for both primary and secondary control loops of the governor. In this study, a BFO algorithm is used to optimizing the integral controller gains for load frequency control of a two area thermal power system without and with IPFC and RFB. To obtain the best convergence performance, new cost function is derive by using the tie-line power and frequency deviations of the control areas and their rates of changes according to time integral. The main function of LFC is to regulate a signal called Area Control Error (ACE), which accounts for error in the frequency as well as the errors in the interchange power with neighboring areas. Conventional Load Frequency Control uses a feedback signal that is either based on the Integral of ACE or is based on ACE and it's Integral. These feedback signals are used to maneuver the turbine governor set points of the generators so that the generated power follows the load fluctuations, however continuously tracking load fluctuations definitely causes wear and tear on governor's equipment, shortens their lifetime, and thus requires replacing them, which can be very costly. In Ref. [24] deals with discrete-time Automatic Generation Control of an interconnected reheat thermal system considering a Area Control Error New (ACEN) based on tie-power deviation, frequency deviation, time error and inadvertent interchange. This controller can effectively regulate time error ($\xi$) and inadvertent interchange accumulations (I). Control Performance Criteria (CPC) has been formerly used to evaluate AGC performance. The Control Performance Standard (CPS) is specifically designed to comply with the performance standards imposed by the North American Electric Reliability Council for equitable operation of an interconnected system. Control Performance Standard (CPS1) and Control Performance Standard 2 (CPS2) are derived from rigorous theoretical basis. CPS1 is a measurement to asses the performance of frequency control in each area. CPS2 is designed to restrain the ACE 10-min average value and in doing so provides a means to limit excessive unscheduled power flows that could results from large ACE. In this paper a novel load frequency controller is present. It is manipulate by a Fuzzy logic system whose rules are design to reduce wear and tear of the equipment and assure its control performance is in compliance with NERC's control performance standards [25,26], CPS1 and CPS2. Considering the power system load frequency control, this paper establishes a fuzzy logic controller to predict the future frequency of the target object, thus forecasting the optimized controller is designed, which follows the CPS performance standards through the fuzzy logic rules. This control structure is a decentralized, integral type controller whose parameter is automatically tuned using Bacterial Foraging Optimization algorithm. The control parameter is reduced to diminish high frequency movement of the speed governor's equipment when the control area has high compliance with NERC's standards. When the compliance is low, the control parameter is raised to the normal

value. This paper adopts CPS1 and CPS2 as input to the fuzzy logic controller and output gain of fuzzy controller adjust control parameter gain (Ki) depending up on NERC's compliance. The simulation results show that the dynamic performance of the system with IPFC and RFB is improve by using the propose controller.

## 2. Problem formulation

The state variable equation of the minimum realization model of '*N*' area interconnected power system [27] may be expressed as

$$\begin{aligned} \dot{x} &= Ax + Bu + \Gamma d \\ y &= Cx \end{aligned} \tag{1}$$

where $x = [x_1^T, \Delta p_{ei} \ldots x_{(N-1)}^T, \Delta p_{e(N-1)} \ldots x_N^T]^T$, $n -$ state vector;

$$n = \sum_{i=1}^{N} n_i + (N-1)$$

$u = [u_1, \ldots u_N]^T = [\Delta P_{C1} \ldots P_{CN}]^T$, $N -$ control input vector;

$d = [d_1, \ldots d_N]^T = [\Delta P_{D1} \ldots P_{DN}]^T$,

$N -$ disturbance input vector;

$y = [y_1 \ldots y_N]^T$, $2N -$ measurable output vector;

where $A$ is system matrix, $B$ is the input distribution matrix, $\Gamma$ is the disturbance distribution matrix, $C$ is the control output distribution matrix, $x$ is the state vector, $u$ is the control vector and $d$ is the disturbance vector consisting of load changes. In order to ensure zero steady state error condition an integral controller may suitability designed for the augmented system. To incorporate the integral function in the controller, the system Eq. (1) is augmented with new state variables defined as the integral of $\mathrm{ACE}_i(\int v_i \mathrm{d}t)$, $i = 1, 2, \ldots N$. The augmented system of the order $(N + n)$ may be described as

$$\dot{\overline{x}} = \overline{A}\overline{x} + \overline{B}u + \overline{\Gamma}d \tag{2}$$

where

$$\overline{x} = \begin{bmatrix} \int v \, \mathrm{d}t \\ x \end{bmatrix} \begin{matrix} \}N \\ \}n \end{matrix} \quad \overline{A} = \begin{bmatrix} 0 & C \\ 0 & A \end{bmatrix} \overline{B} = \begin{bmatrix} 0 \\ B \end{bmatrix} \quad \text{and} \quad \overline{\Gamma} = \begin{bmatrix} 0 \\ \Gamma \end{bmatrix}$$

The problem now is to design the decentralized feedback control law

$$u_i = -k_i^T \overline{y}_i \quad i = 1, 2 \ldots N \tag{3}$$

The control law in Eq. (3) may be written in-terms of $v_i$ as

$$u_i = -k_i \int v_i \mathrm{d}t \quad i = 1, 2 \ldots N \tag{4}$$

where $k_i$ is the integral feedback gain vector, $v_i$ is the scalar control output of area *i*.

## 3. Operating principle of inter-line power flow controller

In its general form the Inter-line Power Flow Controller employs a number of dc-to-ac converters each providing series compensation for a different line. In other words, the Inter-line Power Flow Controller comprises a number of Static Synchronous Series Compensators. The simplest IPFC consists of two back-to-back dc-to-ac converters, which are connects in series with two transmission lines through series coupling transformers and the dc terminals of the converters are connected together via a common dc link as shown in Fig. 1. With this Inter-line Power Flow Controller, in addition to providing series reactive compensation, any converter can be controlled to supply real power to the common dc link from its own transmission line [28]. It can effectively manage the power flow via multi-line transmission system by the injection of proper series voltages in transmission lines with the aid of its inverters.

### 3.1. Power injection model of inter-line power flow controller

In this section, a mathematical model for IPFC is obtained with the power injection model [29] which is helpful in understanding the impact of the IPFC in the power system during the steady state. Furthermore, the IPFC model can easily be incorporated in the power flow model. Usually, in the steady state analysis of power systems, the Voltage Source Converter may be represented as a synchronous voltage source injecting an almost sinusoidal voltage with controllable magnitude and angle. Based on this, the equivalent circuit of IPFC is developed and shown in Fig. 2. Where $V_i$, $V_j$ and $V$ are the complex bus voltages at the buses *i*, *j* and *k* respectively, $\mathrm{Vse_{in}}$ is the complex controllable series injected voltage source, and $\mathrm{Zse_{in}}$ $(n = j, k)$ is the series coupling transformer impedance. The active and reactive power injections at each bus can be easily calculated by representing IPFC as current source. For the sake of simplicity, the resistance of the transmission lines and the series coupling transformers are neglected. The power injections at buses are summarized as

$$P_{\mathrm{inj},i} = \sum_{n=j,k} V_i \mathrm{Vse_{in}} b_{\mathrm{in}} \sin(\theta_i - \theta \mathrm{se_{in}}) \tag{5}$$

$$Q_{\mathrm{inj},i} = -\sum_{n=j,k} V_i \mathrm{Vse_{in}} b_{\mathrm{in}} \cos(\theta_i - \theta \mathrm{se_{in}}) \tag{6}$$

$$P_{\mathrm{inj},n} = -V_n \mathrm{Vse_{in}} b_{\mathrm{in}} \sin(\theta_n - \theta \mathrm{se_{in}}) \tag{7}$$

$$Q_{\mathrm{inj},n} = V_n \mathrm{Vse_{in}} b_{\mathrm{in}} \cos(\theta_n - \theta \mathrm{se_{in}}) \tag{8}$$

where

$V_x = V_x \angle \theta_x \ (x = i, j \text{ and } k)$

$\mathrm{Vse_{in}} = \mathrm{Vse_{in}} \angle \theta \, \mathrm{se_{in}} \ (n = j, k)$.

The equivalent power injection model of an IPFC is shown in Fig. 3. As Inter-line Power Flow Controller neither absorbs nor injects active power with respect to the ac system; the active power exchange between the converters via the dc link is zero, i.e.

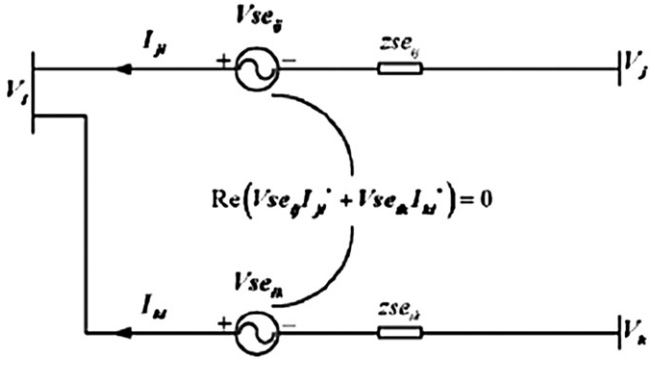


**Fig. 2.** Equivalent circuit of IPFC.

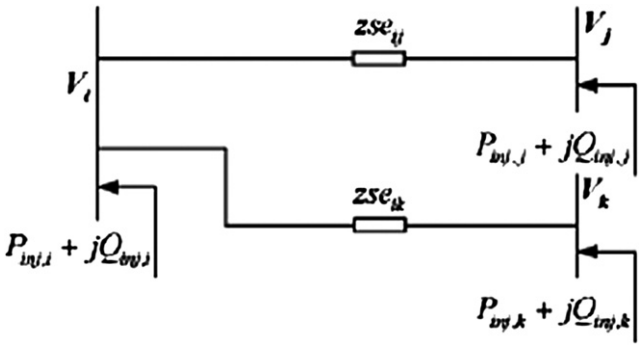


**Fig. 3.** Power injection model of IPFC.

$$\mathrm{Re}\left(\mathrm{Vse}_{ij}I_{ji}^{*} + \mathrm{Vse}_{ik}I_{ki}^{*}\right) = 0 \tag{9}$$

where the superscript * denotes the complex conjugate. If the resistances of series transformers are neglected, Eq. (9) can be written as

$$\sum_{m=i,j,k} P_{\mathrm{inj},m} = 0 \tag{10}$$

Normally in the steady state operation, the IPFC is used to control the active and reactive power flows in the transmission lines in which it is placed. The active and reactive power flow control constraints are

$$P_{ni} - P_{ni}^{\mathrm{spec}} = 0 \tag{11}$$

$$Q_{ni} - Q_{ni}^{\mathrm{spec}} = 0 \tag{12}$$

where $n = j, k$; $P_{ni}^{\mathrm{spec}}, Q_{ni}^{\mathrm{spec}}$ are the specified active and reactive power flow control references respectively, and

$$P_{ni} = \mathrm{Re}\left(V_n I_{ni}^{*}\right) \tag{13}$$

$$Q_{ni} = \mathrm{Im}\left(V_n I_{ni}^{*}\right) \tag{14}$$

Thus, the power balance equations are as follows

$$P_{gm} + P_{\mathrm{inj},m} - P_{lm} + P_{\mathrm{line},m} = 0 \tag{15}$$

$$Q_{gm} + Q_{\mathrm{inj},m} - Q_{lm} + Q_{\mathrm{line},m} = 0 \tag{16}$$

where $P_{gm}$ and $Q_{gm}$ are generation active and reactive powers, $P_{lm}$ and $Q_{lm}$ are load active and reactive powers. $P_{\mathrm{line},m}$, $Q_{\mathrm{line},m}$ are conventional transmitted active and reactive powers at the bus $m = i, j$ and $k$.

## 4. Operating principle of redox flow batteries

The configuration of redox flow battery is shown in Fig. 4. A sulphuric acid solution containing vanadium ions is used as the positive and negative electrolytes, which are stored in respective tanks and circulated to battery cell. The reactions that occur in the battery cell during charging and discharging can be express simply with the following equations [15].

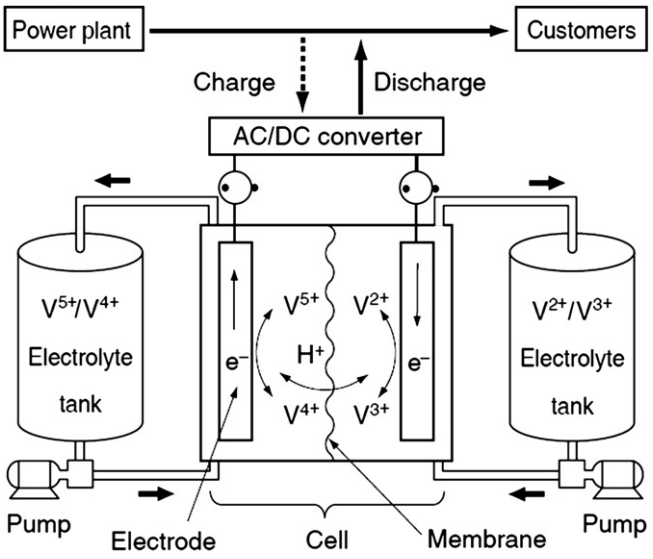


**Fig. 4.** Principles of a redox flow battery.

$$\text{Positive Electrode}: \quad V^{4+} \underset{\text{discharge}}{\overset{\text{charge}}{\rightleftharpoons}} V^{5+} + e^{-} \tag{17}$$

$$\text{Negative Electrode}: \quad V^{3+} + e^{-} \underset{\text{discharge}}{\overset{\text{charge}}{\rightleftharpoons}} V^{2+} \tag{18}$$

The redox flow batteries offer the following features, and are suitable for high capacity systems that differ from conventional power storage batteries. The battery reaction only involves a change in the valence of a vanadium ion in the electrolyte. There are none of the factors which reduce the battery service life seen in other batteries that use a solid active substance, such as loss are electro depositions of the active substance. Further more, operation at normal temperatures ensure less deterioration of the battery materials due to temperature. The system configurations are such that battery output (cell section) and battery capacity (tank section) can be separated, therefore the layout of the sections can be altered according to the place of installation. For example, the tank can be placed underground. The design can be easily modified according to the required output and capacity. The charged electrolyte is stored in separate positive and negative tanks when the battery has been charged, therefore no self-discharge occurs during prolonged stoppage nor is auxiliary power required during stoppage. Furthermore, start-up after prolonged stoppage requires only starting of the pump, thus making start-up possible in only a few minutes. The electrolyte (i.e., the active substance) is sent to the each battery cell from the same tank, therefore the charging state of each battery cell is the same, eliminating the need for special operation such as uniform charging. So that, maintenance is also easy because the electrolyte is relatively safe and the operating are at normal temperature and assures superior environmental safety. Waste vanadium from generating stations can be used so it can be superior recyclability. Furthermore, the vanadium in the electrolyte can be used semi-permanently.

The RFB systems are incorporated in the power system to suppress the load frequency control problem and to ensure an improved power quality. In particular, these are essential for reusable energy generation units, such as wind power and photovoltaic generator units, which need measures for absorption of changes in output and to control flicker and momentary voltage

drop. With the excellent short-time overload output and response characteristics possessed by RFB in particular [16], the effects of generation control and of the absorption of power fluctuation needed for power quality maintenance are expected. The set value of the RFB has to be restored at the earliest, after a load disturbance so that the RFB unit is ready to act for the next load disturbance. The redox flow batteries are capable of ensuring a very fast response and therefore, hunting due to a delay in response does not occur. For this reason, the ΔFi was used directly as the command value for LFC to control the output of RFB.

## 5. System modeling for control design

The redox flow battery and Inter-line Power Flow Controller are found to be superior to the governor system in terms of the faster response against the frequency fluctuations. They are charged with suppressing the peak value of frequency deviations quickly against the sudden load change, subsequently the input to the governor system are updated with the required input for the compensation of the steady state error of the frequency deviations. Fig. 5 shows the model for the control design of RFB and IPFC. Where the dynamics of governor systems are eliminated by setting the mechanical inputs to be constant since the response of governor is much slower than that of RFB or IPFC. The redox flow battery is modeled as an active power source to area1 with a time constant $T_{RFB}$. The IPFC is modeled as a tie line power flow controller with a time constant $T_{IPFC}$. The tie-line power modulated by the IPFC flows into both areas simultaneously with different signs (+ and −) since the responses of power control by the RFB and by the IPFC are sufficiently fast compared to the dynamics of the frequency deviations, the time constants $T_{RFB}$ and $T_{IPFC}$ are regarded as 0 s [5] for the control design. Then the state equation of the system represented by Fig. 5 becomes.

$$\begin{bmatrix} \Delta\dot{F}_1 \\ \Delta\dot{P}_{T12} \\ \Delta F_2 \end{bmatrix} = \begin{bmatrix} -\frac{1}{T_{p1}} & -\frac{k_{p1}}{T_{p1}} & 0 \\ 2\pi T_{12} & 0 & -2\pi T_{12} \\ 0 & \frac{a_{12}k_{p2}}{T_{p2}} & -\frac{1}{T_{p2}} \end{bmatrix} \begin{bmatrix} \Delta F_1 \\ \Delta P_{T12} \\ \Delta F_2 \end{bmatrix} + \begin{bmatrix} \frac{k_{p1}}{T_{p1}} & -\frac{k_{p1}}{T_{p1}} \\ 0 & 0 \\ 0 & \frac{a_{12}k_{p2}}{T_{p2}} \end{bmatrix} \begin{bmatrix} \Delta P_{RFB} \\ \Delta P_{IPFC} \end{bmatrix} \quad (19)$$

Here, from the physical view point it is noted that the IPFC located between two areas is effective to stabilize the inter-area oscillation mode only, and then the RFB which is capable of supplying the energy into the power system should be suitable for the control of the inertia mode.

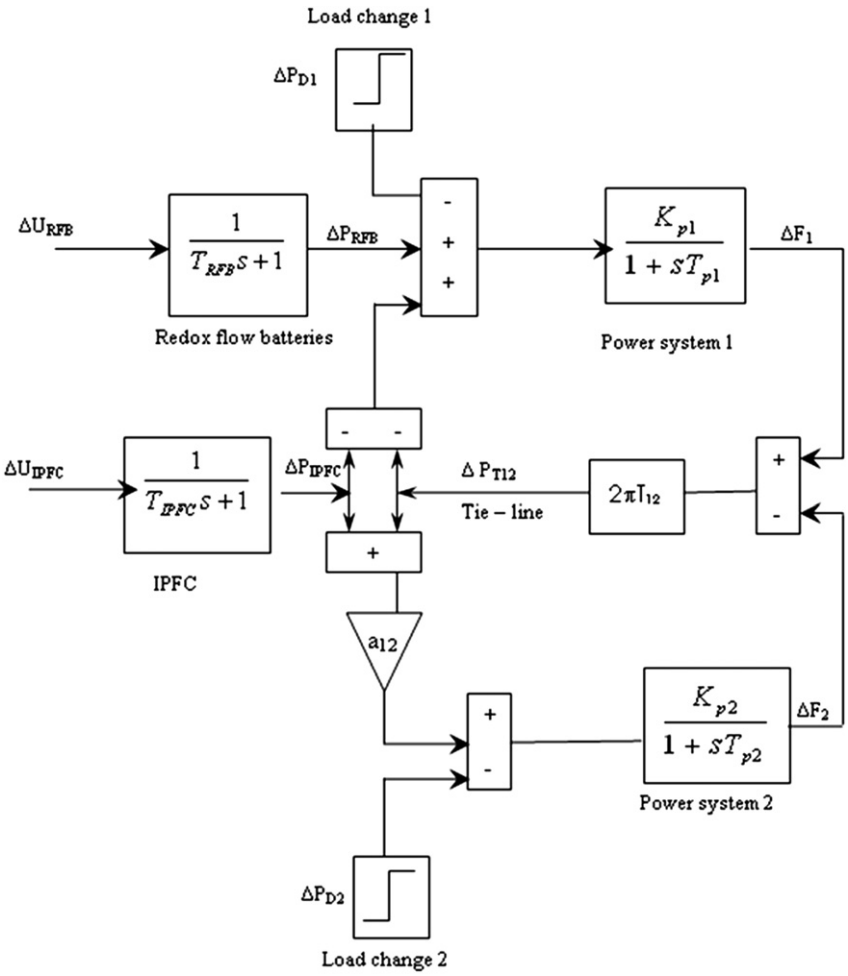


**Fig. 5.** Linearized reduction model for the control design.

### 5.1. Control design of redox flow batteries

The design process starts from the reduction of two area system into one area which represents the Inertia centre mode of the overall system. The controller of RFB is designed in the equivalent one area system to reduce the frequency deviation of inertia centre. The equivalent system is derived by assuming the synchronizing coefficient $T_{12}$ to be large. From the state equation of $\Delta\dot{P}_{T12}$ in Eq. (19)

$$\frac{\Delta\dot{P}_{T12}}{2\pi T_{12}} = \Delta F_1 - \Delta F_2 \tag{20}$$

Setting the value of $T_{12}$ in Eq. (20) to be infinity yields $\Delta F_1 = \Delta F_2$. Next, by multiplying state equation of $\Delta\dot{F}_1$ and $\Delta\dot{F}_2$ in Eq. (19) by $T_{p1}/k_{p1}$ and $T_{p2}/a_{12}\ k_{p2}$ respectively, then

$$\frac{T_{p1}}{k_{p1}}\Delta\dot{F}_1 = -\frac{1}{k_{p1}}\Delta F_1 - \Delta P_{T12} - \Delta P_{\mathrm{IPFC}} + \Delta P_{\mathrm{RFB}} \tag{21}$$

$$\frac{T_{p2}}{a_{12}k_{p2}}\Delta\dot{F}_2 = \frac{-1}{kp_2a_{12}}\Delta F_2 + \Delta P_{T12} + \Delta P_{\mathrm{IPFC}} \tag{22}$$

By summing Eqs. (21) and (22) and using the above relation $\Delta F_1 = \Delta F_2 = \Delta F$

$$\Delta\dot{F} = \frac{\left(-\frac{1}{k_{p1}} - \frac{1}{k_{p2}a_{12}}\right)}{\left(\frac{T_{p1}}{k_{p1}} + \frac{T_{p2}}{k_{p2}a_{12}}\right)}\Delta F + \frac{1}{\left(\frac{T_{p1}}{k_{p1}} + \frac{T_{p2}}{k_{p2}a_{12}}\right)}\Delta P_{\mathrm{RFB}} + C\Delta P_{\mathrm{D}} \tag{23}$$

The load change in this system $\Delta P_{\mathrm{D}}$ is additionally considered, where $C$ is constant, here the control $\Delta P_{\mathrm{RFB}} = -K_{\mathrm{RFB}}\ \Delta F$ is applied then.

$$\Delta F = \frac{C}{S + A + K_{\mathrm{RFB}}B}\Delta P_{\mathrm{D}} \tag{24}$$

$$\text{Where}\quad A = \left(-\frac{1}{k_{p1}} - \frac{1}{k_{p2}a_{12}}\right)\Big/\left(\frac{T_{p1}}{k_{p1}} + \frac{T_{p2}}{k_{p2}a_{12}}\right),$$

$$B = \frac{1}{\left[\frac{T_{p1}}{K_{p1}} + \frac{T_{p2}}{K_{p2}a_{12}}\right]}$$

Since the control purpose of RFB is to suppress the deviation of $\Delta F$ quickly against the sudden change of $\Delta P_{\mathrm{D}}$, the percent reduction of the final value after applying a step change $\Delta P_{\mathrm{D}}$ can be given as a control specification. In Eq. (24) the final values with $K_{\mathrm{RFB}} = 0$ and with $K_{\mathrm{RFB}} \neq 0$ are $C/A$ and $C/(A + K_{\mathrm{RFB}}B)$ respectively therefore the percent reduction is represented by

$$C/(A + K_{\mathrm{RFB}}B)/(C/A) = R/100 \tag{25}$$

For a given $R$, the control gain of RFB is calculated as

$$K_{\mathrm{RFB}} = \frac{A}{\mathrm{BR}}(100 - R) \tag{26}$$

### 5.2. Control design of inter-line power flow controller

The controller for the IPFC is design to enhance the damping of the inter-area mode. In order to extract the inter-area mode from the system Eq. (19), the concept of overlapping decompositions is applied. First, the state variables of the system Eq. (19) are classified into three groups, i.e. $x_1 = [\Delta F_1],\ x_2 = [\Delta P_{T12}],\ x_3 = [\Delta F_2]$ next, the system Eq. (19) is decomposed into two decoupled subsystems. Where the state variable $\Delta P_{T12}$ is duplicated included in both subsystems, which is the reason that this process is called overlapping decompositions. Then, one subsystem which preserves the inter-area mode is represented by.

$$\begin{bmatrix}\Delta\dot{F}_1\\ \Delta\dot{P}_{T12}\end{bmatrix} = \begin{bmatrix}-\frac{1}{T_{p1}} & \frac{-Kp_1}{T_{p1}}\\ 2\pi T_{12} & 0\end{bmatrix}\begin{bmatrix}\Delta F_1\\ \Delta P_{T12}\end{bmatrix} + \begin{bmatrix}\frac{-Kp_1}{T_{p1}}\\ 0\end{bmatrix}[\Delta P_{\mathrm{IPFC}}] \tag{27}$$

It has been proved that the stability of original system is guaranteed by stabilizing every subsystem. Therefore the control scheme of IPFC is designed to enhance the stability of the system Eq. (27) by eigenvalue assignment method. Here let the conjugate eigenvalue pair of the system Eq. (27) be $\alpha \pm j\beta$, which corresponds to the inter-area mode. The control purpose of the IPFC is to damp the peak value of frequency deviation in area 1 after a sudden change in the load demand. Since the system Eq. (27) is the second order oscillation system, the percentage overshoot $M_{p\ (\mathrm{new})}$ can be specified for the control design. $M_{p\ (\mathrm{new})}$ is given as a function of the damping ratio by

$$M_{p(\mathrm{new})} = e^{\left(-\pi\delta/\sqrt{1-\delta^2}\right)} \tag{28}$$

The real and imaginary parts of eigenvalue after the control are expressed by

$$\alpha_s = \delta w_n \tag{29}$$

$$\beta_s = w_n\sqrt{1-\delta^2} \tag{30}$$

where $w_n$ is the undamped natural frequency, by specifying $M_p$ and assuming $\beta_s = \beta$, the desired pair of eigenvalue is fixed. As a result, the eigenvalue assignment method derives to feed back scheme as

$$\Delta P_{\mathrm{IPFC}} = -k_1\Delta F_1 - k_2\Delta P_{T12} \tag{31}$$

The characteristic polynomial of the system Eq. (27) with state feedback, which is given by

$$|\lambda I - (A - BK)| = 0 \tag{32}$$

where state feedback gain matrix $K = [k_1,k_2]$. The desired characteristic polynomial from the specified eigenvalue $(\mu_1,\mu_2)$ is given by

$$(\lambda - \mu_1)(\lambda - \mu_2) = 0 \tag{33}$$

By equating the coefficients of Eqs. (32) and (33) the elements $k_1$, $k_2$ of state feedback gain matrix K are obtained.

## 6. Bacterial foraging optimization technique

### 6.1. Review of bacterial foraging optimization

TheBFO method was introduced by Possino [22] motivated by the natural selection which tends to eliminate the animals with poor foraging strategies and favor those having successful foraging strategies. The foraging strategy is governed by four processes namely Chemotaxis, Swarming, Reproduction and Elimination and Dispersal. Chemotaxis process is the characteristics of movement of bacteria in search of food and consists of two processes namely swimming and tumbling. A bacterium is said to be swimming if it moves in a predefined direction, and tumbling if it starts moving in an altogether different direction. To represent a tumble, a unit length random direction $\varphi(j)$ is generated. Let, "j" is the index of

chemotactic step, "*k*" is reproduction step and "*l*" is the elimination dispersal event. $\theta_i(j,k,l)$, is the position of *i*th bacteria at *j*th chemotactic step *k*th reproduction step and *l*th elimination dispersal event. The position of the bacteria in the next chemotatic step after a tumble is given by

$$\theta^i(j+1,k,l) = \theta^i(j,k,l) + C(i)\varphi(j) \tag{34}$$

If the health of the bacteria improves after the tumble, the bacteria will continue to swim to the same direction for the specified steps or until the health degrades. Bacteria exhibits swarm behavior i.e. healthy bacteria try to attract other bacterium so that together they reach the desired location (solution point) more rapidly. The effect of swarming [22] is to make the bacteria congregate into groups and moves as concentric patterns with high bacterial density. Mathematically swarming behavior can be modeled

$$\begin{aligned} J_{cc}(\theta,P(j,k,l)) &= \sum_{i=1}^{S} J^i cc\left(\theta,\theta^i(j.k.l)\right) \\ &= \sum_{i=1}^{S}\left[-d_{\text{attract}}\exp(-\omega_{\text{attract}})\sum_{m=1}^{p}\left(\theta^m-\theta_m^i\right)^2\right] \\ &+ \sum_{i=1}^{S}\left[-h_{\text{repelent}}\exp\left(-w_{\text{repelent}}\right)\sum_{m=1}^{p}\left(\theta^m-\theta_m^i\right)^2\right] \end{aligned} \tag{35}$$

where $J_{CC}$ – relative distance of each bacterium from the fittest bacterium; $S$ – number of bacteria; $p$ – number of parameters to be optimized; $\theta^m$ – position of the fittest bacteria; $d_{\text{attract}}$, $\omega_{\text{attract}}$, $h_{\text{repelent}}$, $\omega_{\text{repelent}}$ – different co-efficients representing the swarming behavior of the bacteria which are to be chosen properly.

In Reproduction step, population members who have sufficient nutrients will reproduce and the least healthy bacteria will die. The healthier population replaces unhealthy bacteria which get eliminated owing to their poorer foraging abilities. This makes the population of bacteria constant in the *evolution* process. In this process a sudden unforeseen event may drastically alter the evolution and may cause the elimination and/or dispersion to a new environment. Elimination and dispersal helps in reducing the behavior of stagnation i.e., being trapped in a premature solution point or local optima.

### 6.2. Bacterial foraging algorithm

In case of BFO technique each bacterium is assigned with a set of variable to be optimized and are assigned with random values [Δ] within the universe of discourse defined through upper and lower limit between which the optimum value is likely to fall. In the proposed method integral gain $K_{\text{Ii}}$ ($i$ = 1, 2) scheduling, each bacterium is allowed to take all possible values within the range and the cost objective function which is represented by Eq. (45) is minimized. In this study, the BFO algorithm reported in Refs. [22,23] is found to have better convergence characteristics and is implemented as follows.

#### 6.2.1. Step 1 – initialization

1. Number of parameter ($p$) to be optimized.
2. Number of bacterial ($S$) to be used for searching the total region.
3. Swimming length ($Ns$), after which tumbling of bacteria will be undertaken in a chemotacticloop
4. $N_C$ – the number of iteration to be undertaken in a chemotactic loop ($N_C > N_S$)
5. $N_{\text{re}}$ – the maximum number of reproduction to be undertaken.
6. $N_{\text{ed}}$ – the maximum number of elimination and dispersal events to be imposed over bacteria
7. $P_{\text{ed}}$ – the probability with which the elimination and dispersal will continue.
8. The location of each bacterium $P$ ($1-p$, $1-s$, 1) which is specified by random numbers within [−1, 1]
9. The value of $C(i)$, which is assumed to be constant in our case for all bacteria to simplify the design strategy.
10. The value of $d_{\text{attract}}$, $W_{\text{attract}}$, $h_{\text{repelent}}$ and $W_{\text{repelent}}$. It is to be noted here that the value of $d_{\text{attract}}$ and $h_{\text{repelent}}$ must be same so that the penalty imposed on the cost function through "$J_{CC}$" of Eq. (35) well be "0" when all the bacteria will have same value, i.e., they have converged.

After initialization of all the above variables, keeping one variable changing and others fixed the value of "*J*" proposed in Eq. (45) is obtained by running the simulation of system using the parameter contained in each bacterium. The corresponding to the minimum cost, the magnitude of the changing variable is selected. Similar procedure is carried out for other variables keeping the already optimized one unchanged. In this way all the variables of step 1- initialization are obtain and are presented below.

$$\begin{aligned} S &= 6,\ Nc = 10,\ Ns = 3,\ N_{\text{re}} = 15,\ N_{\text{ed}} = 2,\ P_{\text{ed}} \\ &= 0.25,\ d_{\text{attract}} = 0.01,\ w_{attract} = 0.04,\ h_{\text{repelent}} \\ &= 0.01,\ \text{and}\ w_{\text{repelent}} = 10,\ p = 2. \end{aligned}$$

#### 6.2.2. Step 2 – iterative algorithms for optimization

This section models the bacterial population chemotaxis Swarming, reproduction, elimination, and dispersal (initially, $j = k = l = 0$) for the algorithm updating $\theta^i$ automatically results in updating of '*P*'.

1. Elimination – dispersal loop: $l = l + 1$
2. Reproduction loop: $k = k + 1$
3. Chemotaxis loop: $j = j + 1$
   a). For $i$=1, 2…$S$, calculate cost for each bacterium $i$ as follows.
   - Compute value of cost $J(i,j,k,l)$
     Let $J_{sw}(i,j,k,l) = J(i,j,k,l) + J_{cc}(\theta^i(j,k,l),P(j,k,l))$ [i.e., add on the cell to cell attractant effect obtained through Eq. (35) for swarming behavior to obtain the cost value obtained through Eq. (45)].
   - Let $J_{\text{last}} = J_{sw}(i,j,k,l)$ to save this value since a better cost via a run be found.
   - End of for loop.

   b). for $i$ = 1, 2…$S$ take the tumbling/swimming decision.
   - Tumble: generate a random vector $\Delta(i)\in\Re^p$ with each element $\Delta_m(i)$ $m = 1,2,\ldots p$, a random number on [−1,1].
   - Move the position the bacteria in the next chemotatic step after a tumble by Eq. (34)Fixed step size in the direction of tumble for bacterium '*i*' is considered
   - Compute $J(i,j+1,k,l)$ and then let

$$\begin{aligned} J_{sw}(i,j+1,k,l) &= J(i,j+1,k,l) \\ &+ J_{\text{cc}}\left(\theta^i(j+1,k,l),P(j+1,k,l)\right) \end{aligned} \tag{36}$$

   - Swim:
     (i) Let $m = 0$; (counter for swim length)
     (ii) While $m < Ns$ (have not climbed down too long)
   - Let $m = m + 1$

**Table 1**
LFC optimization rules based on CPS.

| Condition | | The state of AGC units |
|---|---|---|
| CPS1 ≥ 100% and CPS2 ≥ 90% | | No optimization adjusting |
| CPS1 < 100% and CPS2 ≥ 90% | ACE*ΔF > 0 | Optimization adjusting |
| | ACE*ΔF < 0 | No optimization adjusting |
| CPS1 ≥ 100% and CPS2 < 90% | | Optimization adjusting |
| CPS1 < 100% and CPS2 < 90% | | Optimization adjusting |

- If $J_{sw}(i,j+1,k,l) < J_{last}$ (if doing better), let $J_{last} = J_{sw}(i,j+1,k,l)$ and let

$$\theta^i(j+1,k,l) = \theta^i(j,k,l) + C(i)\frac{\Delta(i)}{\sqrt{\Delta^T(i)\Delta(i)}} \quad (37)$$

where $C(i)$ denotes step size; $\Delta(i)$ Random vector; $\Delta^T(i)$ Transpose of vector $\Delta(i)$. By using Eq. (37) to compute the new $J(i,j+1,k,l)$ Else let $m = N_s$. This the end of while statement

c). Go to next bacterium $(i+1)$ is selected if $i \neq S$ (i.e. go to b) to process the next bacterium

4. If $j < N_c$, go to step 3. In this case, chemotaxis is continued since the life of the bacteria in not over
5. Reproduction.
   a) For the given $k$ and $l$ for each $i = 1,2\ldots S$, let $J^i_{health} = \min_{j\in\{1\cdots N_c\}}\{J_{sw}(i,j,k,l)\}$ be the health of the bacterium $i$ (a measure of how many nutrients it got over its lifetime and how successful it was in avoiding noxious substance). Sort bacteria in the order of ascending cost $J_{health}$ (higher cost means lower health).
   b) The $S_r = S/2$ bacteria with highest $J_{health}$ values die and other $S_r$ bacteria with the best value split [and the copies that are placed at the same location as their parent].
6. If $k < N_{re}$, go to 2; in this case, as the number of specified reproduction steps have not been reached, so the next generation in the chemotactic loop is to be started
7. Elimination − dispersal: for $i = 1, 2\ldots S$ with probability $P_{ed}$, eliminates and disperses each bacterium [this keeps the number of bacteria in the population constant] to a random location on the optimization domain.

## 7. North American electric reliability council's control performance standards

In 1997, the North American Electric Reliability Council (NERC) proposed new control performance standards [25,26] CPS1 and CPS2 to evaluate the control area performance in normal interconnected power system operation. Each control area is required to monitor its control performance and report its compliance CPS1 and CPS2 to NERC [30,31] at the end of each month.

### 7.1. Control performance standard 1

Control Performance Standard 1 assesses the impact of Area Control Error on frequency over a certain period window or horizon

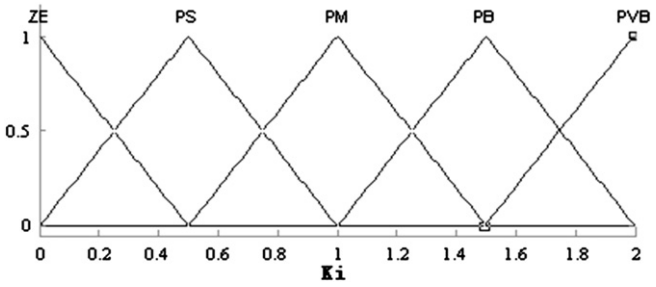


**Fig. 7.** Membership function for the controller outputs ($\alpha$i).

and it is defined as follows: over a sliding certain period, the average of the "clock-min averages" of a control area's Area Control Error divided by "10 times its area frequency bias" times the corresponding "clock- min averages of the interconnection frequency error" shall be less than the square of a given constant $\varepsilon_1$, representing a target frequency bound. This is expressed [32,33]

$$\mathrm{AVG}_{\mathrm{period}}\left[\left(\frac{\mathrm{ACE}_i}{-10\beta_i}\right)_1 \Delta F_i\right] \leq \varepsilon_1^2 \quad (38)$$

where $\mathrm{ACE}_i$: Clock-average of ACE, $\Delta F_i$: the clock- min average of frequency deviation from schedule, $\beta_i$: frequency bias of the control area, $\varepsilon_1$: targeted frequency bound for CPS1, $i$: control area I and $(\cdot)_1$ is the clock 1- min average.

$\varepsilon_1$ is a constant derived the historical frequency record of a control area. It is the root mean square of one- min average frequency deviation from a schedule based on frequency performance over an averaging period of a year. The period $(n)$ is defined as one year for control area evaluation or one month for the report of NERC. To calculate CPS1 ($K_{CPS1}$), a dimensionless compliance factor ($K_{CF}$) is defined as:

$$K_{CF} = \frac{\sum\left[\left(\frac{\mathrm{ACE}_i}{-10\beta_i}\right)_1 \Delta F_1\right]}{n\varepsilon_1^2} \quad (39)$$

CPS1 is then obtained from the following equation:

$$K_{CPS1} = (2 - K_{CF})*100\% \quad (40)$$

The fundamental requirement for CPS1 is that performance, as measured by percentage compliance must be at least 100%.

1. When $K_{CPS1} \geq 200\%$, which means $K_{CF} \leq 0$, there is $\sum(\mathrm{ACE}_1*\Delta F_1) \leq 0$. Under this condition, ACE facilitates the frequency quality.
2. When $100\% \leq K_{CPS1} < 200\%$, which means $0 < K_{CF} \leq 1$, there is $0 \leq \sum[(\mathrm{ACE}_i/-10\beta_i)_1*\Delta F_1] \leq n\varepsilon_1^2$. The Control Performance Standard 1 standard is satisfied.
3. When $K_{CPS1} < 100\%$, which means $K_{CF} > 1$, there is $\sum[(\mathrm{ACE}_i/-10\beta_i)_1*\Delta F_1] > n\varepsilon_1^2$. ACE has exceeded the permitted

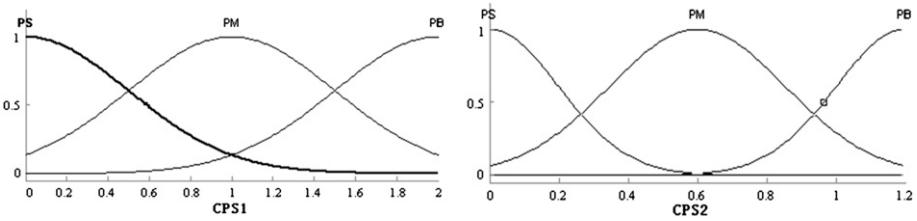


**Fig. 6.** Membership function for the input variables (CPS1, CPS2).

**Table 2**
Fuzzy logic rules.

| CPS2 | CPS1 | | |
|---|---|---|---|
| | PS | PM | PB |
| PS | ZE | PS | PS |
| PM | PS | PB | PM |
| PB | PB | PVB | PVB |

range so that it has a bad effect on the frequency and quality of power grid.

### 7.2. Control performance Standard 2

The Control Performance Standard 2 (CPS2), limits the magnitude of short-term ACE values. It requires the 10-min averages of a control area's ACE be less than a given constant ($L_{10}$), as in the equation below:

$$\mathrm{AVG}_{10\mathrm{min}}(\mathrm{ACE}_i) \le L_{10} \tag{41}$$

where, $L_{10} = 1.65\varepsilon_{10}\sqrt{(-10\beta_i)(-10\beta_s)}$. Note that $\beta_s$ is the summation of the frequency bias settings of all control areas in the considered interconnection, and $\varepsilon_{10}$ is the target frequency bound for CPS2. To comply with this standard, each control area must have its compliance no less than 90%. A compliance percentage is calculated from the following equation:

$$K_{\mathrm{CPS2}} = \frac{\mathrm{AVG}_{10\mathrm{min}}(\mathrm{ACE}_i)}{L_{10}} \tag{42}$$

In order to meet the requirements of the power grid frequency quality, the average ACE value during 10-min in each control region should be in the normal distribution as:

**Table 3**
RFB and IPFC control design results.

| IPFC | RFB |
|---|---|
| 1. Eigenvalue of system Eq. (27)<br>$\lambda 1 = -0.25 + j1.8081$<br>$\lambda 2 = -0.25 - j1.8081$<br>2. Inter-area mode, $M_p = 63.25\%$<br>3. Design specification, $M_{p(new)} = 10\%$<br>4. New Eigenvalue of the system Eq. (27)<br>$\lambda 1(new) = -1.323 + j1.8081$<br>$\lambda 2(new) = -1.323 - j1.8081$<br>5. State Feed back Gain Eq. (31)<br>$[K_1, K_2] = [-0.432, -0.532]$ | 1. Design specification, $R = 2.4$<br>2. RFB gain by Eq. (26), $K_{\mathrm{RFB}} = 0.67$ |

$$\sigma = \varepsilon_{10}\sqrt{(-10\beta_i)(-10\beta_s)} \tag{43}$$

### 7.3. Optimization rules based on control performance standards

Suppose Control Performance Standard 1 $\ge$ 100% and Control Performance Standard 2 $\ge$ 90% to be goal of the LFC control strategy. Table 1 shows LFC optimization rules based on Control Performance Standard.

### 7.4. Fuzzy logic design

Fuzzy logic rules are designed to manipulate the conventional integral- type load frequency control to achieve two objectives: (i) minimize equipments's wear and tear and (ii) comply with NERC, s Control Performance Standard 1 and Control Performance Standard 2. The control structure for each area is

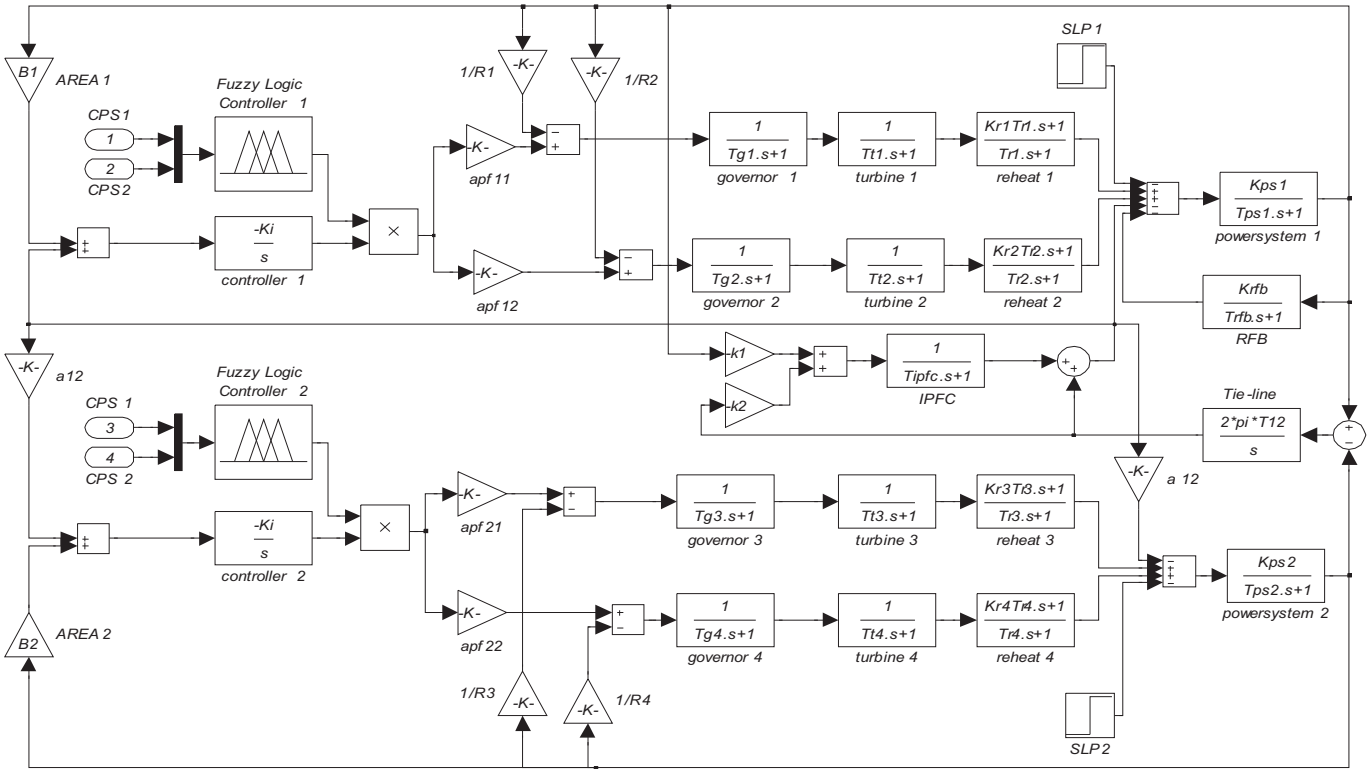


**Fig. 8.** Transfer function model of two-area interconnected thermal reheat power system with IPFC and RFB units.

**Table 4**
Tuned parameter of the control system for three case studies.

| Two area interconnected power system | Feedback gain ($K_i$) | Cost function value ($J$) |
|---|---|---|
| Case: 1 | | |
| Integral controller only | 1.0848 | 0.5879 |
| Case: 2 | | |
| Integral controller with IPFC unit only | 1.1058 | 0.4627 |
| Case: 3 | | |
| Integral controller with IPFC and RFB units | 1.6321 | 0.0146 |

$$u_i = \Delta P_{ci} = \alpha_i K_{il} \int \mathrm{ACE}_i \, \mathrm{d}t \tag{44}$$

where $\Delta P_c$ is the governor set point or raise/lower signal, $K_I$ the integral-control parameter and $\alpha$ is set using fuzzy logic and called fuzzy gain. This paper uses information that reflects compliance with CPS1 and CPS2 as the input to the fuzzy rules. The proposed fuzzy logic will lower the integral gain $K_I$ when the control area has high compliance. On the other hand, that the integral gain $K_I$ will be increased when the compliance with CPS1 of the control area is low. According to the optimized rules from Table 1, the membership functions of CPS1, CPS2 and $\alpha_I$ could be defined as Figs. 6 and 7. Fuzzy rules are summarized in Table 2.

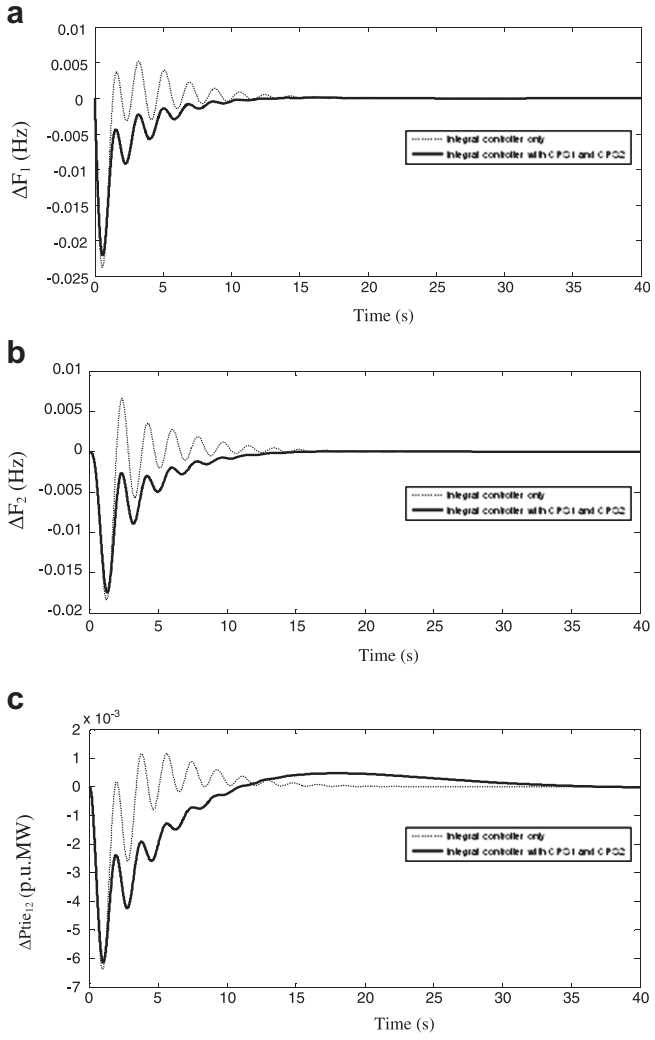


**Fig. 9.** a. Dynamic responses of the frequency deviations of area 1. b. Dynamic responses of the frequency deviations of area 2. c. Dynamic responses of the tie-line power deviations.

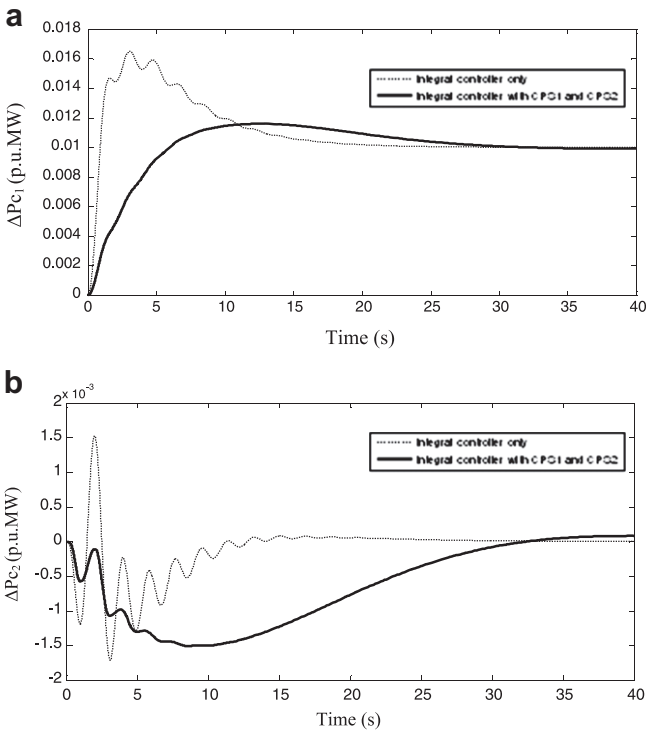


**Fig. 10.** a. Dynamic responses of the control input deviations of area 1. b. Dynamic responses of the control input deviations of area 2.

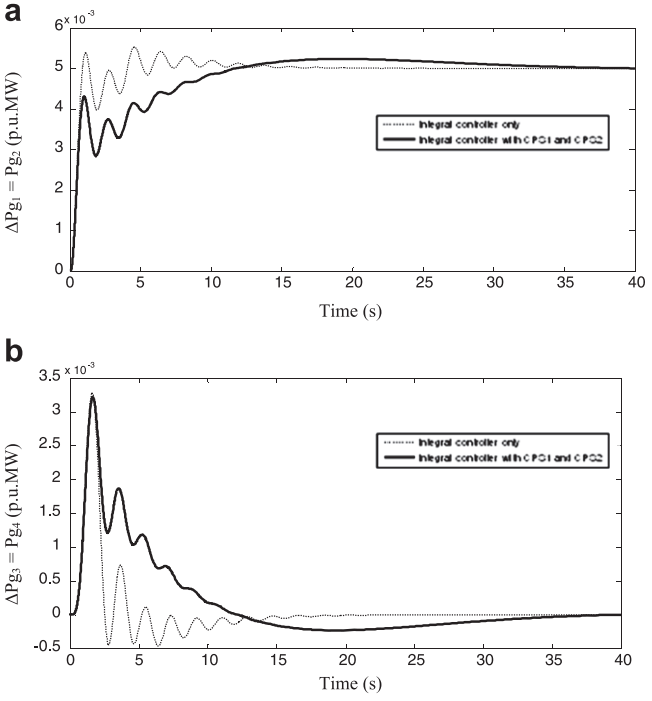


**Fig. 11.** a. Dynamic responses of the required additional mechanical power generation of area 1. b. Dynamic responses of the required additional mechanical power generation of area 2.

## 8. Simulations results and observations

The effect of the propose redox flow batteries coordinate with Interline Power Flow Controller on Load Frequency Control investigate in the two equal area interconnected thermal power system, In each area consists of two reheat units as shown in Fig. 8. In this study the active power model of IPFC controllers is fitted in the tie-line near area1 to examine its effect on the power system performance. Then RFB unit is installing in area 1 and coordinate with IPFC controller for LFC to study its performance of system. The nominal parameters are given in Appendix A. The control parameters of redox flow batteries and Interline Power Flow Controller are design as shown in Table 3. The following object of obtaining the optimal solutions of control inputs is taken an optimization problem, and the novel cost function [34] in Eq. (45) are derive by using the frequency deviations of control areas and tie line power changes. The integral controller gain is tune with BFO algorithm by optimizing the solutions of control inputs. The simulations are realized for 1% step load perturbation in area1. The results are obtained by MATLAB 7.01 software and 50 iterations are chosen for converging to solution in the BFO algorithm.

$$J = \int_0^T \left\{ (\beta_1 \Delta f_1)^2 + (\beta_2 \Delta f_2)^2 + (\Delta P_{tie12})^2 \right\} \quad (45)$$

The BFO algorithm optimal gains of Integral controllers ($K_{I1}$ $K_{I2}$) for three case studies are determining using BFO algorithm. From the simulation, the tuned parameters of the control system are found and shown in Table 4. These controllers are implementing in an interconnected two-area power system without IPFC and RFB, with IPFC only, IPFC coordinate RFB. Relative compliance of the propose controller based LFC schemes to the NERC standards haven been establish for the above power system. In the present work, variation of load in only area1 has been considered. The compliance factor ($K_{CF}$) is compute for 1-h in Eq. (39). Assuming that the response of the controller to the load variations for the year will be similar to that obtained during the sample period of 1-h. According to the compliance factor ($K_{CF}$) value to calculate Control Performance Standard 1, as defined in Eq. (40). In addition, the Control Performance Standard 2, as defined in Eq. (42), has also been computed. CPS1 and CPS2 have two input of fuzzy logic controller, fuzzy logic rules are design according to their Compliance the optimum integral gain $K_I$ changes depends up on fuzzy gain ($\alpha$). It is seen from Figs.9–11; it is evident that the dynamic responses have improved significantly with the use of information that reflects compliance with CPS1 and CPS2. This algorithm will significantly reduce wear and tear of the equipment since movements of the governor set point or raise/lower signal ($\Delta P_c$) generate from the integral controller are less frequent when the control area has high compliance or that values of 1-min average compliance factor (CF) or accumulatively average compliance factor (CF ac) is less than unity. Simulation results are shown in Figs. 12–14; it can be observed that the oscillations in area frequencies and tie-line power deviations have decreases to a considerable extent as compare to that of the system without IPFC controllers. Moreover the RFB locate in area 1which as coordinate with IPFC controllers.

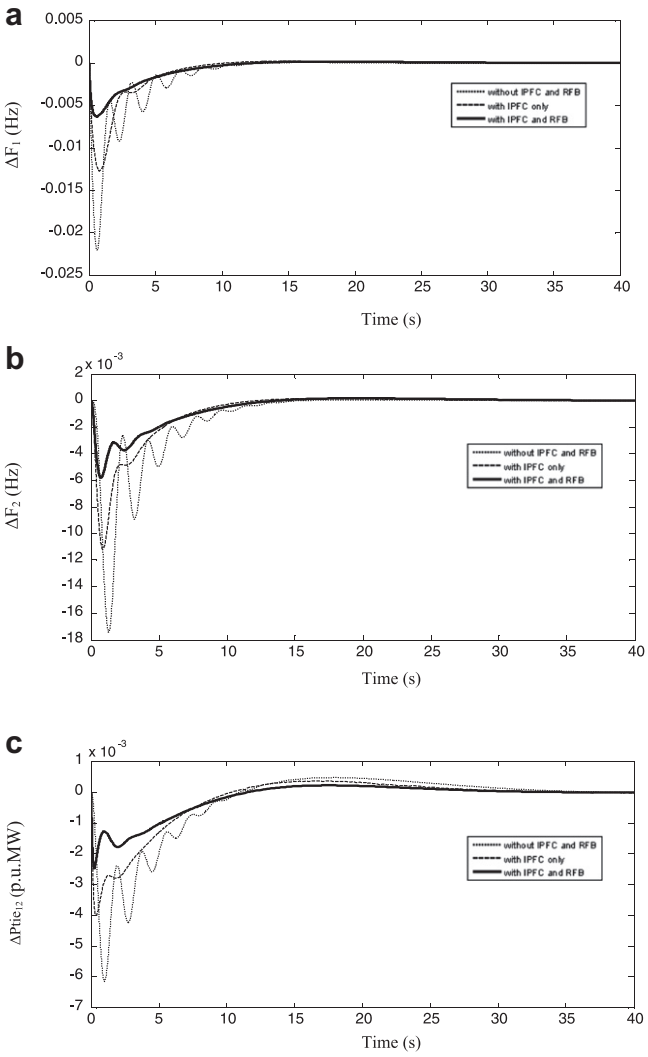


**Fig. 12.** a. Dynamic responses of the frequency deviations of area 1 considering CPS1 and CPS2. b. Dynamic responses of the frequency deviations of area 2 considering CPS1 and CPS2. c. Dynamic responses of the tie line power deviation considering CPS1 and CPS2.

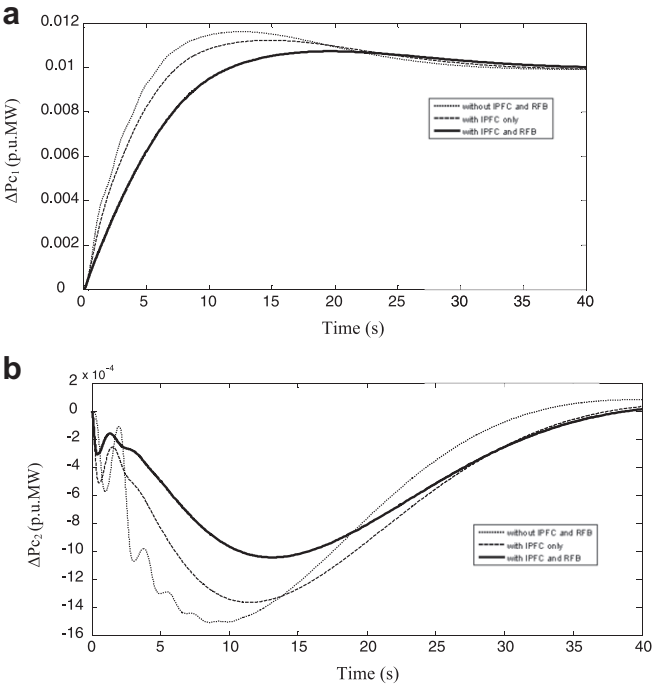


**Fig. 13.** a. Dynamic responses of the control input deviations of area1 considering CPS1 and CPS2. b. Dynamic responses of the control input deviations of area2 considering CPS1 and CPS2.

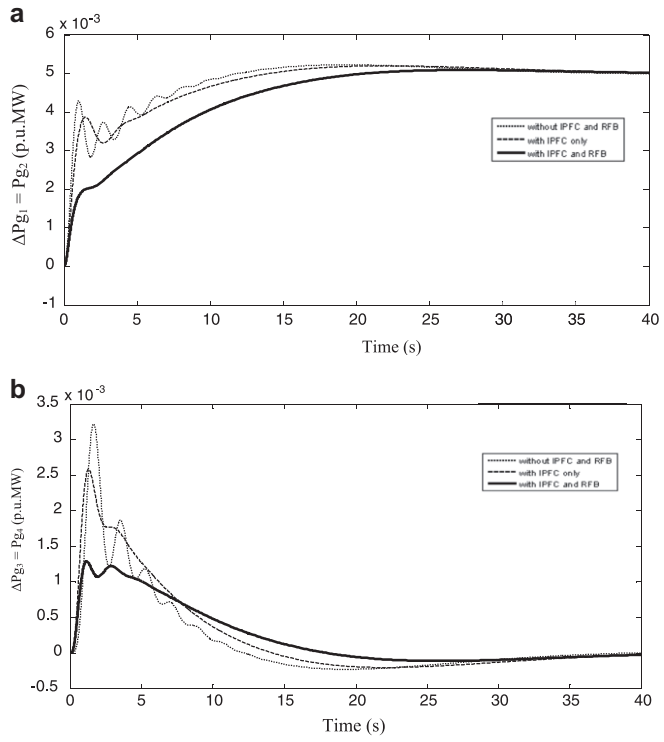


**Fig. 14.** a. Dynamic responses of the required additional mechanical power generation of area1 considering CPS1 and CPS2. b. Dynamic responses of the required additional mechanical power generation of area 2 considering CPS1 and CPS2.

The gain of RFB is calculating using Eq. (26) for given value of speed regulation coefficient ($R$) as shown in Table 3. Redox flow batteries improving the inertia mode oscillation. The settling times and peak over/under shoot for the frequency deviations in each area and tie-line power deviations for three case studies are tabulated in Table 5. Fig. 14 shows the generation responses considering $apf_{11} = apf_{12} = 0.5$ and $apf_{21} = apf_{22} = 0.5$ for three case studies and RFB having $\Delta f_1$ as the control logic signals. As the load disturbances have occurred in area 1, at steady state, the powers generated by generating units in both areas are in proportion to the area participation factors. Therefore, at steady state $\Delta Pg_{1ss} = \Delta Pg_{2ss} = \Delta PD_1{}^{*}apf_{11} = 0.01{*}0.5 = 0.005$ pu.MW and similarly, $\Delta Pg_{3ss} = \Delta Pg_{4ss} = \Delta PD_2 * apf_{21}{=}0 * 0.5{=}0$ pu.MW. From Tables 4 and 5, it can be observe that the controller design using BFO algorithm for two area thermal reheat power system with RFB coordinate with IPFC have not only reduces the cost function but also ensure better stability, as they possesses less over/under shoot and faster settling time when compare with the output response of the system used controller design for the two area-two unit thermal reheat power system without IPFC and RFB units. Moreover the RFB units, suppresses the peak frequency deviations of both areas, and continue to eliminate the steady state error of frequency deviations.

**Table 5**
Comparison of the system performance for the four case studies.

| Two area interconnected power system | Setting time ($\tau_s$) in (s) | | | Peak over/under shoot | | |
|---|---|---|---|---|---|---|
| | $\Delta F_1$ | $\Delta F_2$ | $\Delta P_{tie}$ | $\Delta F_1$ (Hz) | $\Delta F_2$ (Hz) | $\Delta P_{tie}$ (p.u.MW) |
| Case: 1 | | | | | | |
| Integral controller only | 16.37 | 15.19 | 16.48 | 0.0226 | 0.0185 | 0.0064 |
| Case: 2 | | | | | | |
| Integral controller considering CPS1 and CPS2 | 13.76 | 12.72 | 12.44 | 0.0210 | 0.0171 | 0.0061 |
| Case: 3 | | | | | | |
| Integral controller considering CPS1 and CPS2 with IPFC units only | 8.255 | 7.882 | 11.66 | 0.0126 | 0.0108 | 0.0039 |
| Case: 4 | | | | | | |
| Integral controller considering CPS1 and CPS2 with IPFC and RFB units | 5.506 | 7.727 | 7.625 | 0.0059 | 0.0055 | 0.0022 |

## 9. Conclusions

This paper presents a design of load frequency control for interconnected power systems using Bacterial Foraging Optimization algorithm. This algorithm is employ to achieve the optimal parameters of the compensating units. The design objectives are (i) to comply with the North American Electric Reliability council's control performance standards; CPS1 and CPS2, (ii) to reduce wear and tear of generating unit's equipments, and (iii) to design feasible control structure. The control structure is select to be consistent with conventional LFC designs and it is chosen to be a feedback of a signal proportional to the integral of the Area Control Error. The gain of this integral-type controller consists of products of two terms, a conventional control gain and fuzzy gain. The fuzzy gain is set using fuzzy logic rules. Which are developed to comply with NERC's standards and to manipulate the generator's set points only if need be to reduce excessive maneuvering and hence minimize the cost of operation and maintenance associate with LFC. A sophisticated Load Frequency Control by redox flow batteries coordinate with Interline Power Flow Controller has proposed for a two area interconnected Reheat Thermal Power System. This BFO algorithm has faster converging algorithm and will reduce computational burden. A control strategy has been proposed to adjust the voltage of IPFC which in turn controls the inter-area tie-line power flow. Simulation results reveal that the first peak frequency deviation of both areas and tie-line power oscillations following sudden load disturbances in either of the areas can be suppress a controlling the series voltage of IPFC. Moreover, the tie-line power flow control by an IPFC unit has to be efficient and effective for improving the dynamic performance of load frequency control of inter connected power system than that of the system without IPFC controllers. The advantages of the expect RFB over existing power system in the LFC applications were examined. RFB contributes a lot in promoting the efficiency of overall generation control through the effect of the use in load leveling and the assurance of LFC capacity after overload characteristic and quick responsiveness. Simulation results reveal that the design concept of damping the inertia mode and inter-area mode, the co-ordinate control is effective to suppress the frequency deviation of two area system simultaneously. It may be therefore be conclude that, the redox flow batteries with a sufficient margin of LFC capacity absorbs the speed governor capability in excess of falling short of the frequency bias value and tie-line power flow control by an Inter line Power Flow Controller be expect to be utilize as a new ancillary service for the stabilization of the tie-line power oscillations even

under the congestion management environment of the power system.

## Acknowledgement

The authors wish to thank the authorities of Annamalai University, Annamalainagar, Tamilnadu, India for the facilities provided to prepare this paper.

## Appendix A

(A) Data for thermal reheat power system [27,32,33].

Rating of each area = 2000 MW, Base power = 2000 MVA, fo = 60 Hz, $R_1 = R_2 = R_3 = R_4 = 2.4$ Hz/p.u.MW, $T_{g1} = T_{g2} = T_{g3} = T_{g4} = 0.08$ s, $T_{r1} = T_{r2} = T_{r1} = T_{r2} = 10$ s, $T_{t1} = T_{t2} = T_{t3} = T_{t4} = 0.3$ s, $K_{p1} = K_{p2} = 120$ Hz/p.u.MW, $T_{p1} = T_{p2} = 20$ s, $\beta_1 = \beta_2 = 0.425$ p.u.MW/Hz, $K_{r1} = K_{r2} = K_{r3} = K_{r4} = 0.5$, $2\pi T_{12}$=0.545 p.u.MW/Hz, $a_{12} = -1$, $\Delta P_{D1} = 0.01$ p.u.MW, $\varepsilon_1 = 18$ mHz, $\varepsilon_{10} = 5.7$ mHz.

(B) Data for IPFC [12]: $T_{IPFC} = 0.01$ s;
(C) Data for RFB [16]: $T_{RFB} = 0$ s.

## References

[1] O.I. Elgerd, Electric Energy Systems Theory: An Introduction, McGraw-Hill, New York, 1982.
[2] P. Kundur, Power System Stability and Control, McGraw-Hill, New York, 1994.
[3] H. Shayeghi, H.A. Shayanfar, A. Jalili, Energy Convers. Manage. 50 (2) (2009) 344–353.
[4] P. Ibraheem, D. Kumar, P. Kothari, IEEE Trans. Power Syst. 20 (1) (2005) 346–357.
[5] Issarachai Ngamroo, Yasunori Mitani, Kiichiro Tsuji, IEEE Trans. Appl. Superconduct. 9 (2) (1999) 113–122.
[6] I. Ngamroo, J. Tippayachai, S. Dechanupaprittha, Electr. Power Energy Syst. 28 (2006) 513–524.
[7] Yong Hua Song, Allan T. Johns, Flexible AC Transmission Systems (FACTS), Institution of Electrical Engineers, London, 1999.
[8] M. Noroozian, L. Angquist, M. Ghandhari, G. Andersson, IEEE Trans. Power Deliv. 12 (4) (1997) 1629–1634.
[9] Y. Xiao, Y.H. Song, Y.Z. Sun, IEEE Trans. Power Syst. 17 (4) (2002) 943–950.
[10] I. Alomoush Muwaffaq, IEEE Trans. Power Syst. 18 (2003) 1173–1180.
[11] R. Strzelecki, G. Benysek, Z. Fedyczak, Interline power flow controller-probabilistic approach, in: IEEE 33rd Annual IEEE Power Electronic Specialists Conference, 2 (2002) 1037–1042.
[12] L. Gyugi, K. Sen, C.D. Schauder, IEEE Trans. Power Deliv. 14 (3) (1999) 1115–1123.
[13] Chen Jianhong, T. Lie Tjing, D.M. Vilathgamuwa, IEEE Power Eng. Soc. 1 (2002) 521–525.
[14] S. Teerathana, A. Yokoyama, Y. Nakachi, M. Yasumatsu, An optimal power flow control method of power system by interline power flow controller (IPFC), in: Proceeding on the 7th International Power Engineering Conference, Singapore, 2005, 1–6.
[15] N. Tokuda, Development of a redox flow battery system, Japan Society of energy and resources, in: The conference of Energy System and Economy and Environment (1998).
[16] K. .Enomoto, T. .Sasaki, T. .Shigematsu, H. Deguchi, IEEE J. Trans. Power Eng. 122-B (4) (2002) 554–560.
[17] C.H. Liang, C.Y. .Chung, K.P. .Wong, X.Z. .Duan, C.T. .Tse, IET. Generat. Transmis. Distrib. 1 (2007) 253–260.
[18] Y. Shi, R.C. Eberhart, Parameter selection in PSO, in: Proceedings of 7th Annual Conference on Evolutionary Computation (1998) 591–601.
[19] M. Dorigo, M. .Birattari, T. .Stutzle, IEEE. Comput. Intelligen. Magaz. (2007) 28–39.
[20] Ghoshal, Electr. Power Syst. Res. 70 (2004) 115–127.
[21] M.A. Abido, IEEE Trans. Energy Convers. 17 (3) (2002) 406–413.
[22] K.M. Passino, IEEE Control Syst. Magaz. 22 (3) (2002) 52–67.
[23] Janardan Nanda, S. Mishra, Lalit Chandra Saikia, IEEE Trans. Power Syst. 24 (2) (2009) 602–609.
[24] M.L. Kothari, J. Nanda, D.P. Koathari, D. Das, IEEE Trans. Power Syst. 4 (2) (1989) 730–738.
[25] G. Gross, J.W. Lee, IEEE Trans. Power Syst. 16 (3) (2001) 520–526.
[26] M.J. Yao, R.R. Shoults, R. Kelm, IEEE Trans. Power Syst. 15 (2) (2000) 852–857.
[27] I.A. Chidambaram, S. Velusami, Electr. Power Compon. Syst. 33 (12) (2005) 1313–1331.
[28] N.G. Hingorani, L. Gyugyi, Understanding FACTS; Concepts and Technology of FACTS, first ed., IEEE Press, John Wiley and Sons Inc., New York, 2000.
[29] A.V. Naresh Babu, S. Sivanagaraju, Ch. Padmanabharaju, T. Ramana, ARPN J. Eng. Appl. Sci. 5 (10) (2010) 1–4.
[30] North American Electric Reliability Council (NERC), Performance standard training document, in: Operating Manual, North America, 1996, pp. 1–20.
[31] Northern Regional Load Dispatched Center (online). Available: http//www.nrldc.org.
[32] Ali Feliachi, Electr. Power Syst. Res. 73 (2005) 101–106.
[33] X.J. Liu, J.W. Zhang, CPS compliant fuzzy neural network load frequency control, in: American Control Conference, 2009, 2755–2760.
[34] Ogata Katsubiko, Modern Control Engineering, Prentice Hall of India, New Delhi, 2010.